Received: 1 March 2024 | Revised: 29 July 2024 | Accepted: 6 August 2024

DOI: 10.1002/asmb.2887

RESEARCH ARTICLE

WILEY

Stock market bubbles and the forecastability of gold returns and volatility

David Gabauer[1] | **Rangan Gupta**[2] | **Sayar Karmakar**[3] | **Joshua Nielsen**[4]

[1]Data Analysis Systems, Software Competence Center, Hagenberg, Austria

[2]Department of Economics, University of Pretoria, Hatfield, South Africa

[3]Department of Statistics, University of Florida, Gainesville, Florida, USA

[4]Boulder Investment Technologies, LLC, Boulder, Colorado, USA

Correspondence
Sayar Karmakar, Department of Statistics, University of Florida, 230 Newell Drive, Gainesville, FL 32601, USA.
Email: sayarkarmakar@ufl.edu

Funding information
National Science Foundation, Grant/Award Number: DMS 2124222

Abstract

In this article, multi-scale LPPLS confidence indicator approach is used to detect both positive and negative bubbles at short-, medium-, and long-term horizons for the stock markets of the G7 and the BRICS countries. This enables detecting major crashes and rallies in the 12 stock markets over the period of the 1st week of January, 1973 to the 2nd week of September, 2020. Similar timing of strong (positive and negative) LPPLS indicator values across both G7 and BRICS countries was also observed, suggesting interconnectedness of the extreme movements in these stock markets. Next, these indicators were utilized to forecast gold returns and its volatility, using a method involving block means of residuals obtained from the popular LASSO routine, given that the number of covariates ranged between 42 and 72, and gold returns demonstrated a heavy upper tail. The finding was, these bubbles indicators, particularly when both positive and negative bubbles are considered simultaneously, can accurately forecast gold returns at short- to medium-term, and also time-varying estimates of gold returns volatility to a lesser extent. The results of this paper have important implications for the portfolio decisions of investors who seek a safe haven during boom-bust cycles of major global stock markets.

KEYWORDS

bubbles, forecasting, gold, returns, stock markets, volatility

1 | INTRODUCTION

There exists an already large, and still growing, literature associated with the forecasting of gold price and/or returns based on a large spectrum of macroeconomic, financial, and behavioral predictors that rely on a wide array of linear and nonlinear univariate or multivariate models (see for example, Pierdzioch et al.,[1–6] Aye et al.,[7] Hassani et al.,[8] Sharma,[9] Gupta et al.,[10] Bonato et al.,[11] Nguyen et al.,[12] Dichtl,[13] Plakandaras and Ji[14]). This is not surprising, since, the role of gold as a "safe haven" relative to extreme equity market movements in particular, and also in comparison to other assets (bonds, (crypto-)currencies, and even commodities in the wake of its recent financialization post the Global Financial Crisis (GFC),[15] is quite well-established (see for example, Baur and Lucey,[16] Baur and McDermott,[17] Reboredo,[18,19] Agyei-Ampomah et al.,[20] Gürgün and Ünalmis,[21] Beckmann et al.,[22] Low et al.,[23] Balcilar et al.,[24] Ji et al.,[25] Tiwari et al.,[26] Lahiani et al.[27]). Naturally, accurate forecasting of gold price and/or returns is of paramount importance to investors in designing their optimal portfolios involving gold due to its ability to offer diversification and hedging benefits during periods of turmoil and heightened uncertainties in conventional financial markets.

Against this backdrop, the objective of this paper is to make the first attempt to forecast weekly gold returns over the period of the 1st week of January, 1973 to the 2nd week of September, 2020, based on the information content of indicators that capture stock market bubbles in the G7 (Canada, France, Germany, Italy, Japan, the United Kingdom (UK), and the United States (US)), and the BRICS (Brazil, Russia, India, China and South Africa). As far as detecting bubbles are concerned, we not only use the log-periodic power law singularity (LPPLS) model, originally developed by Johansen et al.[28,29] and Sornette,[30] for both positive (upward accelerating price followed by a crash) and negative (downward accelerating price followed by a rally) bubbles, but we then apply the Multi-Scale LPPLS Confidence Indicators (MS-LPPLS-CI) of Demirer et al.[31] to characterise positive and negative bubbles at different time scales, that is, short-, medium-, and long-term.

At this stage, it is important to highlight the following issues associated with our forecasting exercise. First, we consider bubble indicators in the stock market as predictors, since traditionally, the safe haven property of gold has been analyzed in relation to extreme behavior of equity markets. Besides, there is ample evidence that contagion in asset markets are primarily driven by equity markets (see the detailed discussions in Caporin et al.[32,33]). Second, bubbles are detected by applying the MS-LPPLS-CI approach on the stock price-dividend ratios, given the present-value theoretical framework of Campbell and Shiller,[34] whereby the importance of dividends as a fundamental for pricing equities is well-established. Determining a single fundamental for other assets (bonds, cryptocurrencies, exchange rates, commodities) markets is not necessarily straight-forward, as they have been found to be driven by many possible predictors (see for example, Çepni et al.,[35] Hollstein et al.,[36] Koki et al.,[37] Salisu et al.,[38] and references cited therein), and hence it becomes difficult to detect bubbles as deviations from a key fundamental based on our approach. Third, we identify both positive and negative bubbles across the 12 countries, which is not possible otherwise based on other available tests of detecting bubbles (see, Balcilar et al.,[39] Zhang et al.,[40] and Sornette et al.[41] for detailed reviews). And then, we use them in the predictive model on their own and together to gauge the possible asymmetric predictive impact on gold returns, given that crash and recovery can carry different information for the gold market as a safe haven. The expectation is that positive bubbles are likely to be a stronger predictor than the negative ones. In the same vein, the time-scale of the bubble indicators could also matter for the forecasting of gold returns, given that market agents (investors, speculators and traders) are likely to react differently to the disaggregate information of short-, medium- and long-term indicators at various investment (forecasting) horizons. This line of reasoning emanates from the Heterogeneous Market Hypothesis,[42] which states that different classes of market participants populate asset markets and differ in their sensitivity to information flows at different time horizons. Given this, gold traders and speculators are likely to be sensitive to short- and medium-term bubbles, whereas investors are possibly going to be more concerned with long-term bubbles. Finally, the choice of the G7 countries is driven by availability of data spanning nearly half a century (1973-2020), which in turn allows us to study many historically important asset markets-related boom-bust cycles (such as, the "Black Monday" in 1987, the Dot-com bubble, the Asian Financial Crisis (AFC) and the GFC).* Note that, when we combine the G7 with the BRICS, our data sample is restricted to over two decades: 1999–2020. Besides the perspective related to coverage of data, the G7 and the BRICS together account for majority of global net wealth and output, and hence, the extreme movements in their asset markets is likely to have a worldwide spillover effect.[44,45] In this regard, the usage of weekly, rather than daily, data allows us to include the information of the equity market bubble indicators in our econometric model simultaneously and match with gold returns, as we no longer need to be concerned about the time-differences in the respective opening and closing times of both the stock and gold markets.

As we deal with many predictors, that is, negative and positive bubble indicators for three time-scales: short-, medium-, and long-term, depending on whether we look at the G7 or the G7 and BRICS together respectively, the cost of overparameterization (due to high number of predictors) in a standard predictive regression framework, and hence the associated poor out-of-sample performance, cannot be overlooked. Given this, it is standard practice to resort to a least absolute shrinkage and selection operator (LASSO)-based estimation technique, as proposed by Tibshirani.[46] But, just like in the case of many assets, gold returns also tend to exhibit heavy-tails,† which causes parametric methods to fail in providing reasonably accurate forecasts. To deal with this issue, a quantile-based method with large number of predictors is utilized by us, following the work of Karmakar et al.,[47] which has been shown by these authors to outperform many of its competitors within the similar class of models. These authors chose to obtain prediction intervals of (time-aggregated) forecasts, conditioned on a large number of (stochastic) covariates and a very general (even possibly heavy-tailed) error structure, based on quantiles of suitably blocked data. However, instead of providing prediction intervals, we will employ the block-division strategy, and focus on point forecasts of gold returns using the mean of these blocks.

While, in line with the safe haven property, the primary focus is on gold returns, the role of bubbles in having a second-moment impact cannot be ignored, since crash or rally of the stock markets can serve as negative (positive) news, and

could result in higher or lower trading activity, which in turn might translate into higher (lower) volatility in the gold market.[48] Realizing this, as an additional analysis, we also delve into, for the first time, the role of the positive and negative bubble indicators across the three time-scales for the G7 and the BRICS in forecasting the conditional volatility of gold prices.[‡] Note that, the metric of volatility is obtained by fitting a Time-Varying Parameter Generalized Autoregressive Conditional Heteroskedasticity (TVPGARCH) model of Karmakar and Roy[51] to weekly gold returns, which in turn has been shown to outperform its corresponding constant parameter version.[52]

The remainder of the article is organized as follows: Section 2 presents the multi-scale LPPLS and forecasting methodologies of gold returns and volatility, Section 3 outlines the data used, and discusses the results involving both bubble detection and forecasting, and Section 4 concludes.

2 | METHODOLOGIES

In this section, we will be outlining the technical details of our econometric methods utilized. In this regard, first we will discuss the MS-LPPLS-CI approach applied to the natural logarithm of ratio of the aggregate stock price of a specific country relative to the corresponding dividends generated in that particular equity market ($ln(p_t)$), in detecting short-, medium-, long-term positive and negative stock market bubbles. In the process, we will start off with the LPPLS methods, and follow that up with how we generate the underlying confidence indicators across the time-scales. Having done these, that is, after explaining how we obtain the underlying predictors (bubbles indicators), we will then present the predictive model used to forecast gold returns. Finally, as we not only forecast gold returns, but also its volatility, we will provide details of the econometric model used to obtain the estimates of conditional volatility of gold returns.

2.1 | Detecting stock market bubbles

Given the LPPLS model as follows, we use the stable and robust calibration scheme developed by Filimonov and Sornette[53]:

$$E[\ln p(t)] = A + B(t_c - t)^m + C(t_c - t)^m \cos(\omega \ln (t_c - t)^m - \phi), \tag{1}$$

where, ln denotes the natural logarithm, the parameter t_c represents the critical time (the date of the termination of the bubble), A is the expected log-value of the observed time-series (i.e., log price-dividend ratio in our case) at time t_c, B is the amplitude of the power law acceleration, C is the relative magnitude of the log-periodic oscillations, and the exponent of the power law growth is given by m. The frequency of the log-periodic oscillations is given by ω and ϕ represents a phase shift parameter.

Following Filimonov and Sornette,[53] (1) is reformulated to reduce the complexity of the calibration process by eliminating the nonlinear parameter ϕ and expanding the linear parameter C to be $C_1 = C\cos\phi$ and $C_2 = C\sin\phi$. The new formulation can be written as:

$$E[\ln p(t)] = A + Bf_m(t) + C_1 g_m(t) + C_2 h_m(t), \tag{2}$$

where

$$\begin{aligned} f_m(t) &= (t_c - t)^m, \\ g_m(t) &= (t_c - t)^m \cos[\omega \ln(t_c - t)], \\ h_m(t) &= (t_c - t)^m \sin[\omega \ln(t_c - t)]. \end{aligned}$$

Let $p_i = p(\tau_i), f_i = f_m(\tau_i), g_i = g_m(\tau_i)$ and $h_i = h_m(\tau_i)$. To estimate the three nonlinear parameters: $\{t_c, m, \omega\}$, and four linear parameters: $\{A, B, C_1, C_2\}$, we fit equation (2) to the log of the price-dividend ratio and minimize the following sum of squared residuals:

$$F(t_c, m, \omega, A, B, C_1, C_2) = \sum_{i=1}^{N} \left[\ln p_i - A - Bf_i - C_1 g_i - C_2 h_i\right]^2, \tag{3}$$

where N denotes the length of the input time series, and each τ_i represents a specific point in time corresponding to an observed value in the price time series p_i. In (3), the dependence of $F(\cdots)$ on m and ω are how we define f_i, g_i and h_i by the means of the functions $f_m(\cdot), g_m(\cdot)$, and $h_m(\cdot)$. Since the estimation of the three nonlinear parameters depend on the four linear parameters, we have the following cost function:

$$F_1(t_c, m, \omega) = \min_{A,B,C_1,C_2} F(t_c, m, \omega, A, B, C_1, C_2) = F(t_c, m, \omega, \hat{A}, \hat{B}, \hat{C}_1, \hat{C}_2). \tag{4}$$

The four linear parameters are estimated by solving the optimization problem:

$$\{\hat{A}, \hat{B}, \hat{C}_1, \hat{C}_2\} = \arg \min_{A,B,C_1,C_2} F(t_c, m, \omega, A, B, C_1, C_2) \tag{5}$$

which can be done analytically by solving the following matrix equation:

$$\begin{pmatrix} N & \sum f_i & \sum g_i & \sum h_i \\ \sum f_i & \sum f_i^2 & \sum f_i g_i & \sum f_i h_i \\ \sum g_i & \sum f_i g_i & \sum g_i^2 & \sum g_i h_i \\ \sum h_i & \sum f_i h_i & \sum g_i h_i & \sum h_i^2 \end{pmatrix} \begin{pmatrix} \hat{A} \\ \hat{B} \\ \hat{C}_1 \\ \hat{C}_2 \end{pmatrix} = \begin{pmatrix} \sum \ln p_i \\ \sum f_i \ln p_i \\ \sum g_i \ln p_i \\ \sum h_i \ln p_i \end{pmatrix}. \tag{6}$$

Next, the three nonlinear parameters can be determined by solving the following nonlinear optimization problem:

$$\{\hat{t}_c, \hat{m}, \hat{\omega}\} = \arg \min_{t_c,m,\omega} F_1(t_c, m, \omega). \tag{7}$$

We use the sequential least squares programming (SLSQP) search algorithm (Kraft, 1988) to find the best estimation of the three nonlinear parameters $\{t_c, m, \omega\}$.

For each LPPLS model fit, the estimated parameters are filtered against established thresholds (discussed in the next sub-section, See (8)) and the qualified fits are taken as a fraction of the total number of positive or negative fits. A positive fit has estimated $B < 0$ and a negative fit has estimated $B > 0$.

2.2 | Multi-scale LPPLS confidence indicator

The LPPLS-CI, introduced by Sornette et al.,[54] is used to measure the sensitivity of bubble patterns in the log price-dividend ratio time series of each country. The larger the LPPLS-CI, the more reliable the LPPLS bubble pattern and vice versa. It is calculated by calibrating the LPPLS model to shrinking time windows by shifting the initial observation t_1 forward in time towards the final observation t_2 with a step dt.

Following the work of Demirer et al.,[31] we incorporate bubbles of varying multiple time-scales into this analysis. We sample the time series in steps of five trading days. We create the nested windows $[t_1, t_2]$ and iterate through each window in steps of two trading days. In this manner, we obtain a weekly resolution from which we construct the following indicators:

- Short-term bubble: A number $\in [0, 1]$ which denotes the fraction of qualified fits for estimation windows of length $dt := t_2 - t_1 \in [30 : 90]$ trading days per t_2. This indicator is comprised of $(90 - 30)/2 = 30$ fits.
- Medium-term bubble: A number $\in [0, 1]$ which denotes the fraction of qualified fits for estimation windows of length $dt := t_2 - t_1 \in [90 : 300]$ trading days per t_2. This indicator is comprised of $(300 - 90)/2 = 105$ fits.
- Long-term bubble: A number $\in [0, 1]$ which denotes the fraction of qualified fits for estimation windows of length $dt := t_2 - t_1 \in [300 : 745]$ trading days per t_2. This indicator is comprised of $(745 - 300)/2 = 223$ fits.

Filter Conditions: After calibrating the model, the following filter conditions are applied to determine which fits are qualified.

$$m \in [0.01, 0.99],$$
$$\omega \in [2, 15],$$

$$t_c \in [\max(t_2 - 60, t_2 - 0.5(t_2 - t_1)), \min(252, t_2 + 0.5(t_2 - t_1))], \tag{8}$$
$$O := \frac{\omega}{2\pi} \ln\left(\frac{t_c - t_1}{t_c - t_2}\right) > 2.5,$$
$$D := \frac{m|B|}{\omega|C|} > 0.5.$$

For every time step, we calibrate the LPPLS model 30 times to obtain the short-term LPPLS-CI, 105 times for the medium term LPPLS-CI and 223 times for the long term LPPLS-CI. For each time scale (short, medium, long) we determine whether or not the fits are qualified. A qualified fit is one that meets the criteria outlined in the list of "filter conditions". Then the proportion of qualified fits is defined as LPPLS-CI value for that time-step. For the convenience of the reader, here we provide an illustration for the long-term LPPLS constituent fits for South Africa for nearly 3 years of data.

The strength of LPPLS bubble structure in their respective time scales are captured by the CI or confidence indicators across the short, medium and long-time scales. For example, an indication of bubble formation in the last three months can be conjectured if the short-term CI takes on a large value, while the medium and long-term CI values are small. For our application, this provides an appropriate setting to examine the short and long-term predictability patterns in bubbles using the corresponding confidence indicators at different time scales.

2.3 | The forecasting model

Here, we describe the basics of the methodology for forecasting a time series data, that is, gold returns (and volatility) using a large number of covariates (i.e., our time-scale-based bubble indicators for the G7, and the G7 plus the BRICS). We have two gold returns datasets involving the 72 predictors of the G7 plus the BRICS of length 1120 data points, and a larger dataset of 2489 observations involving only the 42 predictors associated with the G7. Our goal here is to see whether these covariates can improve accuracy of a standard benchmark time series model of gold returns (and volatility). For simplicity, we use the Autoregressive (AR(1)) model as the benchmark, but our results were similar for higher order AR models (which are available upon request from the authors).

Mathematically speaking, we wish to compare between the following models:

$$\text{Model 1: } y_t = a_0 + a_1 y_{t-1} + e_t \text{ versus Model 2: } y_t = a_0 + a_1 y_{t-1} + \sum_{j=1}^{p} \beta_j x_{t,j} + e_t.$$

When the number of covariates p is large, it is usual to adopt a LASSO-based estimation technique. However, as econometric data routinely exhibit heavier tails, a completely parametric method might fail to provide reasonably accurate forecasts. To deal with the latter problem, Zhou et al.[55] provided a quantile-based method for constructing prediction intervals for low-dimensional regression. The authors therein chose to obtain prediction intervals for the time-aggregated forecasts $y_{T+1} + \ldots, y_{T+h}$, and this is what we also do in our paper. However, instead of providing prediction intervals, we will focus on point forecasts of $(y_{T+1} + \ldots, y_{T+h})/h$. Note that, such an aggregated mean is common for econometric data when it comes to deciding the evaluation metric (see for example, Stărică,[56] Fryzlewicz et al.,[57] Karmakar et al.,[58] and relevant references therein). The theoretical aspects of the papers by Zhou et al.[55] or Karmakar et al.[47] find an interesting advantage of time-aggregation. When h is even moderately large, future aggregated means start to behave typically in accordance with the law of large numbers and thus, pave the path for systematic forecasting with very reasonable guarantees on accuracy.

However, this quantile-based method was only meant for low-dimensional regressions. More recently, this was extended to a high-dimensional regression scenario by Karmakar et al.[47] Moreover, the performance of this new method was able to substantially outperform the prediction intervals reported in Müller and Watson,[59] and some other popular existing forecasting methods.[§]

Given the above, we can now describe our method in a systematic fashion for Model 2. Note that, for Model 1, standard AR forecasting routines were utilized.

1. Obtain the Lasso estimate of $\kappa = (a_0, a_1, \beta_1, \cdots, \beta_p)$ by the means of LASSO regression

$$\hat{\kappa} = \arg\min\left(\sum_{t=1}^{T} (y_t - a_0 - a_1 y_{t-1} - \sum_{j=1}^{p} \beta_j x_{t,j})^2 + \lambda(|a_0| + |a_1| + \sum_j |\beta_j|) \right).$$

2. Use $\hat{e}_i = y_i - \hat{y}_i$, where $\hat{y}_i$ is the fit from Step 1 to then obtain the block means

$$\tilde{e}_{i,h} = \frac{\hat{e}_1 + \ldots + \hat{e}_h}{h}.$$

3. Final forecasts for $(y_{T+1} + \ldots, y_{T+h})/h$ are

$$(\hat{y}_{T+1} + \ldots, \hat{y}_{T+h})/h + \text{mean}(\tilde{e}_{,h}).$$

In our forecasting exercise, we also shrink the a_0 and a_1 parameters. Note that in the results segment, we only describe the findings for the most regularized choice of λ as done in the R program `cv.glmnet`.

2.4 | Estimating volatilites via the TVPGARCH model

We describe how to obtain the volatility estimate from the log-returns of the gold data, using the TVPGARCH model as follows:

$$y_t \sim N(0, \sigma_t^2) \text{ with } \sigma_t^2 = \alpha_0(t/n) + \alpha_1(t/n) y_{t-1}^2 + \beta_1(t/n)\sigma_{t-1}^2. \tag{9}$$

To estimate the time-varying parameter functions $\alpha_0(\cdot)$, $\alpha_1(\cdot)$ and $\beta_1(\cdot)$, we follow the kernel-based method as described in Karmakar et al.[47] We use a suitable choice of kernel, K, and bandwidth, $b_n \in [0, 1]$, to obtain the parameter estimation of: $\theta = (\alpha_0, \alpha_1, \beta)$, as follows:

$$\hat{\theta}_{b_n}(t) = \underset{\theta \in \Theta}{\text{argmin}} \sum_{i=1}^{n} K((t - i/n)/b_n) \ell(y_i, X_i, \theta), \qquad t \in [0, 1], \tag{10}$$

where $\ell(\cdot)$ is the corresponding negative log-likelihood or quasi log-likelihood for estimating the GARCH parameters, X_i denotes the covariates, which in this case will be y_{i-1}, given that we use an univariate GARCH model. In particular, for this problem of estimation, ℓ takes the following form:

$$\ell(y_i, X_i, \theta') = -\frac{1}{2}\log(\sigma_i^2) + y_i^2/\sigma_i^2 \text{ with } \sigma_i^2 = \alpha_0 + \alpha_1 y_{i-1}^2 + \beta_1 \sigma_{i-1}^2,$$

and we choose the Epanechnikov Kernel for K. Finally, with the estimated function $\alpha_0(\cdot)$, $\alpha_1(\cdot)$ and $\beta_1(\cdot)$, we can compute $\hat{\sigma}^2$. Once we obtain the estimate of the volatility, we now replace the same instead of the gold returns in our forecasting model described in the preceding sub-section, and compare it with the AR(1) benchmark.

3 | DATA AND FINDINGS

3.1 | Data

The daily gold price data in US dollars, which is then converted to weekly values by taking averages over the number of trading days, is obtained from the London Bullion Market Association (now known simply as LBMA).[¶] We compute weekly log-returns, which are then matched with the weekly bubble indicators. The latter are derived based on the natural

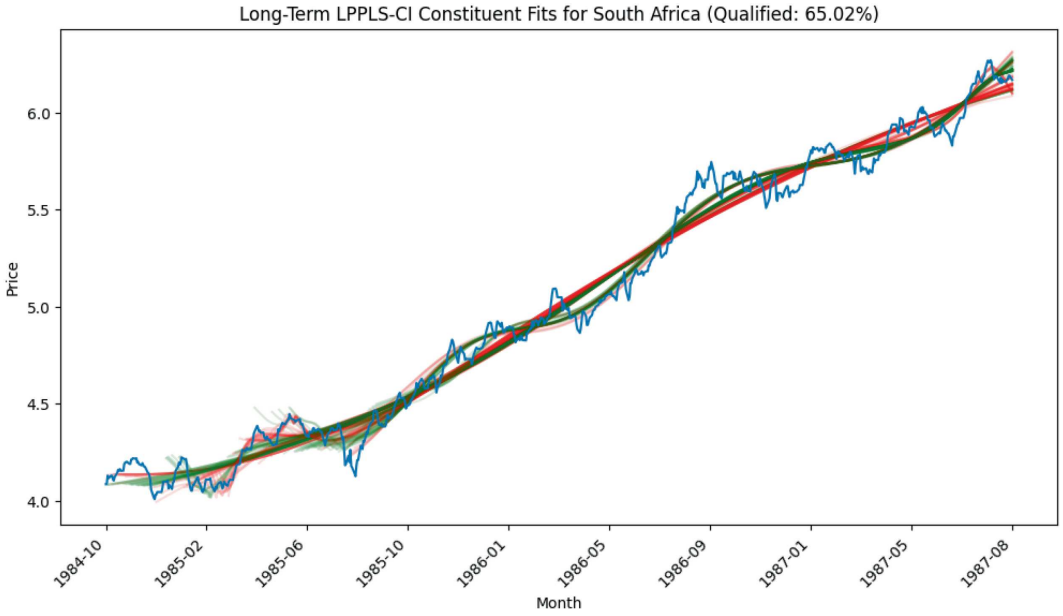

FIGURE 1 LPPLS-CI consitutent fits for South Africa (qualified 65.02 % at t_2 = Aug 31, 1987). Here green and red fits indicate qualified and unqualified fits. LPPLS-CI is proportion of green fits.

logarithmic values of the daily price-dividend ratio (i.e., stock price relative to dividend) of the 12 countries, with the data on overall stock market prices and dividend series individually, in their local currencies, are obtained from Refinitiv Datastream. While data for different countries have different starting points,[#] the need to use balanced data for the G7 and the G7 plus BRICS cases results in us covering the weekly periods of 1st week of (7th) January, 1973 to 2nd week of (13th) September, 2020, and 2nd week of (14th) February, 1999 to 2nd week of (13th) September, 2020, respectively. The gold returns, and the derived volatility[‖] from the TVPGARCH model have been plotted in Figure 1.

3.2 | Detection of bubbles

In this section, we discuss each of the multi-scale LPPLS-CI values for the G7 and the BRICS countries sampled at a weekly frequency. Results are displayed in Figure 2. The short-, medium-, and long-term indicators are displayed in different colors (green, purple, and red, respectively), and the log price-to-dividend ratio is displayed in black. Higher LPPLS-CI values from a corresponding scale indicate that the LPPLS signature is present for many of the fitting windows to which the model was calibrated. As such, it is more reliable. The long-term positive LPPLS-CI (red line in Figure 2) comprised of 223 single LPPLS model fits spanning the fitting windows of size 300 to 745 observations; this corresponds to nearly 3 years of data. Due to the larger calibration time-period, we anticipate that large indicator values will occur less frequently at this scale than they would for smaller scales. The medium-term LPPLS-CI (purple line in Figure 2) uses 105 fits and spans the fitting windows of size 90 to 300 observations, that is, comprising of a little over one year of data. Finally, the short-term LPPLS-CI (green line in Figure 2) uses 30 fits from the fitting windows of size 30 to 90 observations, and hence represents just a month. As can be seen from Figure 2, this scale produces the most signals. It can also be inferred that the smallest crashes or rallies are signaled from this scale. However, we still can see small corrections immediately following a strong short-term LPPLS-CI value.

3.2.1 | The case of the G7

For the long-term LPPLS-CI, we see four strong positive regimes and 2 strong negative regimes. The first is observed in Canada, France, Germany, Italy, the UK and the US from 1973 to 1974. This strong indicator value preceded one of the worst global market downturns since the Great Depression lasting from January, 1973 through December 1974. This crash

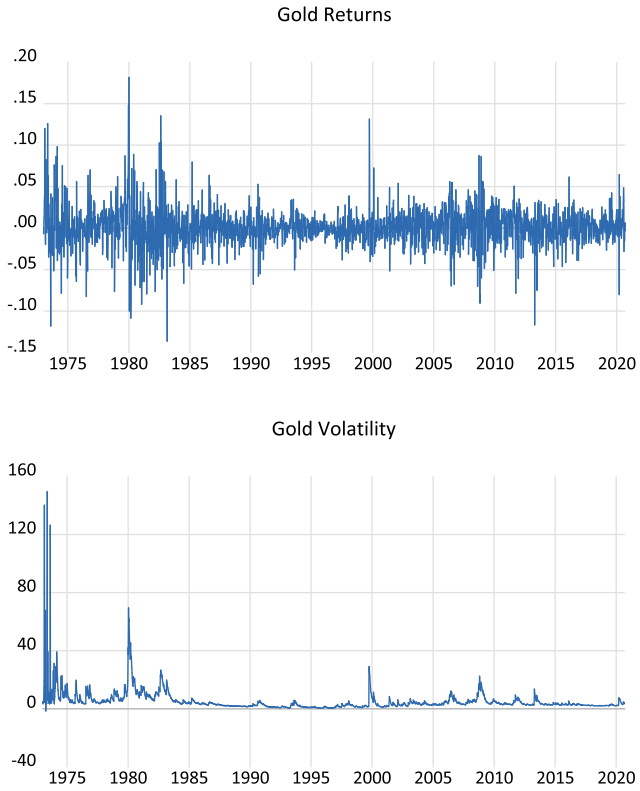

FIGURE 2 Gold returns and volatility data plot.

came on the heels of the collapse of the Bretton Woods system, and the devaluation of the dollar from the Smithsonian Agreement. A bounce-back is observed following this crash for the same countries. Next, we see a strong positive long-term LPPLS-CI value preceding "Black Monday" (on the 19th of October, 1987) in Canada, Japan, the UK and the US. For the UK, the LPPLS-CI value recorded prior to the Black Monday is the largest observed in our data-set. Third, we have the Dot-com bubble, which reached its peak in March, 2000, and has corresponding strong positive large-scale LPPLS-CI values for Canada, Japan and the US. Immediately following the Dot-com crash, we see a strong negative LPPLS-CI value in Canada, France, Italy, the UK and the US. This represents the rally after the sell-off involving the technological stocks. Lastly, we can see strong positive LPPLS-CI values for Canada, France, Italy and the US preceding the stock market sell-off in 2015-2016. This period coincided with the devaluation of the Chinese yuan, the continued Greek debt crisis, effects from the quantitative easing measures coming to an end the US in October, 2014, and the "Brexit" in June, 2016. Furthermore, it can be observed that strong positive/negative medium-term LPPLS-CI values are more ubiquitous, and fore run strong positive/negative long-term LPPLS-CI values previously described.

In addition to these events, we also see a few unique positive/negative short-term LPPLS-CI values, particularly preceding the GFC. It can also be inferred from Figure 2 that the smallest crashes/rallies are signaled from this scale. However, we still can see small corrections immediately following a strong short-term LPPLS-CI value. It is also interesting to notice that the short-term indicators precede the medium-term indicators, just as the latter did in comparison to the long-term ones. This adds support to the finding from Demirer et al.[31] suggesting the presence of the maturation of the bubble towards instability across several distinct time-scales. Lastly, this scale exhibits the least amount of co-occurrence across the countries analyzed in this study, that is, this scale seems to exhibit the most idiosyncratic signals when compared to the two other scales.

3.2.2 | The case of the BRICS

For the BRICS countries, we observe two strong long-term positive LPPLS-CI regimes. The first precedes the GFC, especially for Brazil, China and India. The second emerges between 2014 and 2018. There are notably fewer long-term negative

LPPLS-CI values, with the most apparent negative bubble for this scale occurring after the GFC, capturing recovery. We see pronounced LPPLS-CI values for both positive and negative bubbles everywhere we observed the spikes in the long-term indicators. In addition, we see strong positive medium-term LPPLS-CI values emerge prior to strong long-term LPPLS-CI values leading up to the GFC. For all BRICS countries except Russia, we see a small rally signaled by a negative short-term LPPLS-CI value in late 2002, likely associated with the recover following the technological stocks sell-off. We plot this data in Figures A1–A3 in the Appendix.

3.2.3 | Summary

Given that an asset's volatility increases with the square-root of time as time increases, we can say that smaller time-scales are best-suited for detecting smaller crashes or rallies, and that larger time-scales are better for detecting larger crashes or rallies. This intuition is confirmed by empirically observing the results from Figures 2 and 3. Long-term scales produces fewer signals, but appear to pick-up larger crashes or rallies, while the smaller scales produces more signals that precede smaller crashes or rallies. We also observed similar timing of strong (positive and negative) LPPLS-CI values across both the G7 and BRICS countries, lending to the idea that extreme movements in the stock markets of these major global economies tend to be aligned. Overall, these empirical findings support the claims that the LPPLS framework is a flexible tool for detecting bubbles across different time-scales. In addition, both positive and negative bubbles indicators at the three scales, seem to carry unique information, and hence should serve as important predictors when considered separately, rather than aggregating them across the nature of the bubble and the scales.

3.3 | Forecasting results

Having discussed the evolution of the bubbles indicators for the G7 and the BRICS, we now concentrate on our forecasting experiment obtained from the benchmark AR(1) model, and the benchmark augmented with the 42 predictors in case of the G7, and 72 for the G7 plus the BRICS scenario, with the large model estimated using the approach of Karmakar et al.[47] discussed above. Keeping the nested nature of the models in mind, our evaluation metric here is the p-value of the Clark and West[61] test of forecast comparison, based on the rolled over pseudo-out-of sample forecasts at $h = 1, 2, 4, 8$, and 12, based on training length $T = 100, 250, 500$, and 1000, withe latter used only for the G7 case.

We can make the following remarks about the derived results from Tables 1–3:[**]

- For the case of gold returns, the gains by incorporating the bubbles indicators is significant across various training lengths, at $h = 1, 2$, and 4, irrespective of whether we use the G7 indicators or the G7 plus the BRICS. In fact, significant forecasting gains can also be observed at $h = 8$ when we consider the case of the G7 countries only;
- Given that the bubble indicators across the 12 countries considered were found to be highly synchronized, we computed dynamic total connectedness index (TCI) using the time-varying parameter vector autoregressive (TVP-VAR) based connectedness approach of Antonakakis et al.[62††] for the cases of the G7 only and the G7 plus the BRICS. This connectedness measure indicates the degree of network interconnectedness of the bubble indicators, and provides us with six TCIs each for the G7 and the G7 plus the BRICS, which basically corresponds to the six different bubbles indicators of the countries that were included in six separate TVP-VARs to obtain the TCIs for the two country groups. As can be seen from Table 2, the TCIs, just like with the individual bubbles indicators, continue to produce a similar picture in terms of the forecasting of gold returns;
- Compared to log-returns, the gains for forecasting the estimated gold returns volatility is statistically weaker, as significance is primarily detected at the 10% level (unlike at 1% and 5% for gold returns). Nevertheless, the weaker significant gains tend to cover all the forecasting horizons considered, particularly for the case of the G7 plus the BRICS, and under lower training lengths;
- In general, we can conclude, in line with the safe haven intuition, that financial market bubbles tend to forecast gold returns more accurately than its corresponding volatility, relative to a benchmark AR model.

Next we focus on trying to analyze, whether the positive bubbles indicators involving crashes, tends to perform better than their negative counterparts in forecasting gold returns and its volatility, given that economic agents are expected to invest relatively more in gold during periods of financial market turmoils, than recoveries.

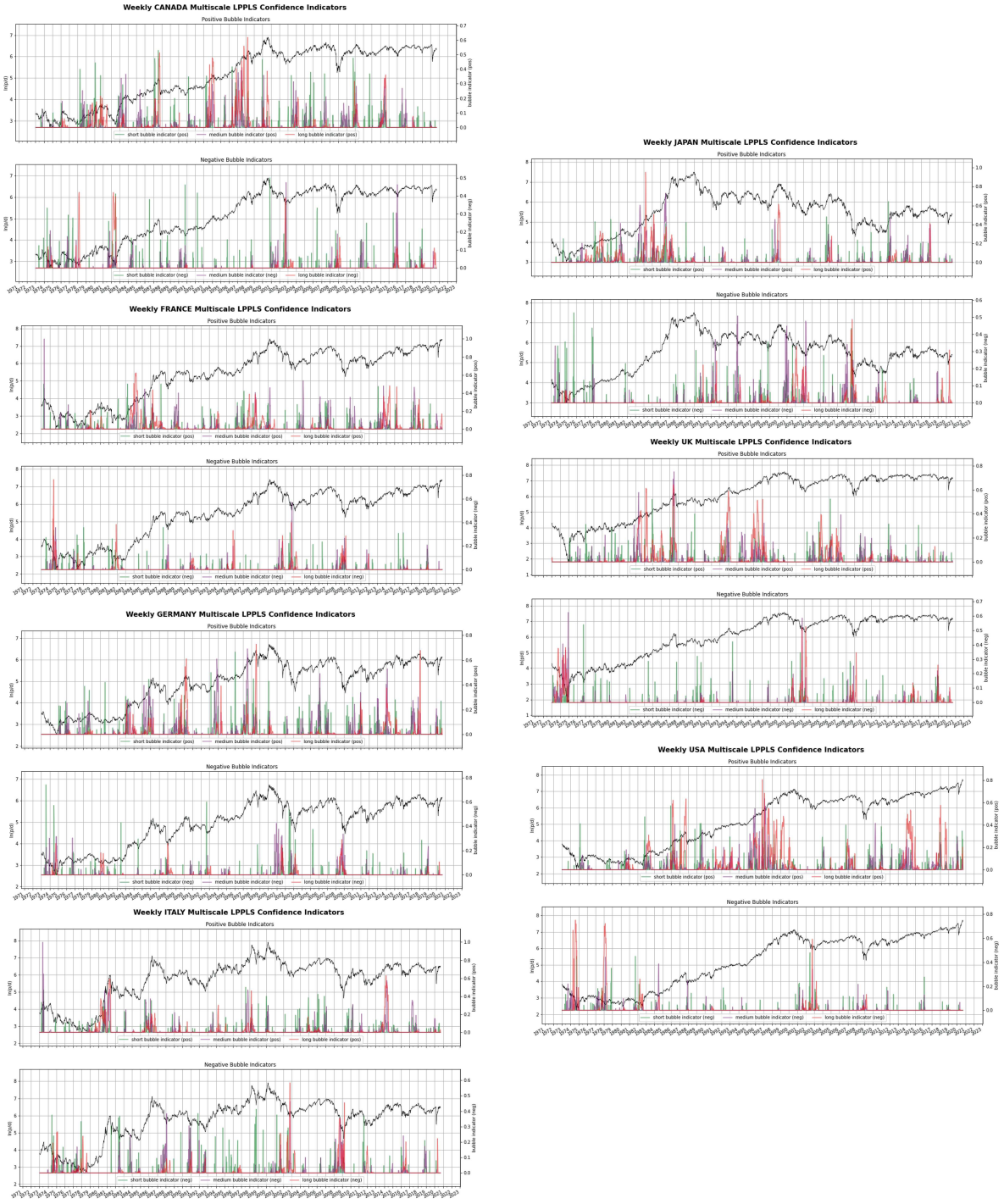

FIGURE 3 G7 Weekly Multi-Scale LPPLS-CI.

The results reported in Tables 4 and 5 for the two subsets, that is, positive and negative multi-scale LPPLS-CIs are not drastically different in their respective abilities to produce forecasting gains relative to the AR(1) model for both gold returns and volatility. However, the model with the positive bubbles indicators generally tends to outperform the one with negative indicators, especially in terms of the lower p-values associated with the CW test in the case of gold returns. But to confirm this statistically, we perform the Diebold and Mariano[63] test of equality of forecasts across the two non-nested models in Tables 6 and 7. As can be seen from below, the DM test generally tends to provide weak evidence in favor of choosing one category of indicator over the other. In other words, it is better to combine the information content of both crashes and recovery when predicting movements in the gold market.

TABLE 1 CW *p*-values for gold returns forecasting based on the multi-scale LPPLS-CI of the G7, and the G7 plus the BRICS.

	G7+BRICS			G7			
Horizon	$T = 100$	$T = 250$	$T = 500$	$T = 100$	$T = 250$	$T = 500$	$T = 1000$
$h = 1$	6.37e−08	4.42e−07	6.41e−07	3.36e−06	1.14e−06	4.65e−13	9.78e−10
$h = 2$	0.0007	0.0019	0.0068	0.0139	0.0010	2.56e−05	1.42e−05
$h = 4$	0.0314	0.0033	0.0314	0.7244	0.7428	4.90e−05	0.0012
$h = 8$	0.4582	0.6995	0.4771	0.8057	0.0177	0.0285	0.2975
$h = 12$	0.8335	0.7945	0.3684	0.4509	0.8890	0.8075	0.8145

TABLE 2 CW *p*-values for gold returns volatility forecasting based on the TCI of the multi-scale LPPLS-CI of the G7, and the G7 plus the BRICS.

	G7+BRICS			G7			
Horizon	$T = 100$	$T = 250$	$T = 500$	$T = 100$	$T = 250$	$T = 500$	$T = 1000$
$h = 1$	1.64e−08	4.45e−07	6.42e−07	1.25 e−05	1.03e−06	4.67e−13	9.79e−10
$h = 2$	0.0006	0.0006	0.0068	0.0003	0.0016	2.57e−05	1.38e−05
$h = 4$	0.0040	0.0061	0.0314	0.0087	0.0059	4.80e−05	0.0012
$h = 8$	0.5138	0.6899	0.4771	0.0225	0.0291	0.0295	0.2991
$h = 12$	0.3765	0.7777	0.3684	0.3387	0.5240	0.8083	0.9224

TABLE 3 CW *p*-values for gold returns volatility forecasting based on the multi-scale LPPLS-CI of the G7, and the G7 plus the BRICS.

	G7+BRICS			G7			
Horizon	$T = 100$	$T = 250$	$T = 500$	$T = 100$	$T = 250$	$T = 500$	$T = 1000$
$h = 1$	0.0698	0.0886	0.9319	0.0525	0.0653	0.2653	0.1678
$h = 2$	0.07393	0.0845	0.7856	0.0387	0.0614	0.3574	0.1917
$h = 4$	0.0652	0.0908	0.6954	0.0742	0.0752	0.4759	0.2659
$h = 8$	0.0489	0.0629	0.4005	0.1255	0.1101	0.6605	0.2945
$h = 12$	0.0594	0.0849	0.4167	0.1459	0.1303	0.7963	0.2862

TABLE 4 CW *p*-values for gold returns forecasting based on the positive only and negative only multi-scale LPPLS-CI of the G7, and the G7 plus the BRICS.

	G7+BRICS			G7			
Horizon	$T = 100$	$T = 250$	$T = 500$	$T = 100$	$T = 250$	$T = 500$	$T = 1000$
$h = 1$ positive	1.70e−08	4.45-07	1.57-06	2.53-06	1.14-06	4.65e−13	9.82e−10
$h = 1$ negative	2.02e−08	4.51e−07	0.0003	4.09e−06	1.149e−06	4.66e−13	9.81e−10
$h = 2$ positive	0.0006	0.0007	0.2174	0.0005	0.0010	2.56e−05	1.41e−05
$h = 2$ negative	0.0007	0.0005	0.1352	0.0207	0.0331	2.55e−05	1.42e−05
$h = 4$ positive	0.0053	0.00655	0.4476	0.0139	0.7428	4.90e−05	0.0012
$h = 4$ negative	0.0084	0.0019	0.9149	0.7030	0.7142	5.12e−05	0.0012
$h = 8$ positive	0.5139	0.7032	0.3544	0.0159	0.0177	0.0291	0.3008
$h = 8$ negative	0.0759	0.7785	0.9072	0.8062	0.7795	0.0285	0.3128
$h = 12$ positive	0.3948	0.7801	0.3026	0.3306	0.8890	0.80754	0.8228
$h = 12$ negative	0.6363	0.9125	0.8119	0.5540	0.9299	0.8068	0.7766

TABLE 5 CW *p*-values for gold returns volatility forecasting based on the positive only and negative only multi-scale LPPLS-CI of the G7, and the G7 plus the BRICS.

	g7+BRICS			g7			
Horizon	$T = 100$	$T = 250$	$T = 500$	$T = 100$	$T = 250$	$T = 500$	$T = 1000$
$h = 1$ positive	0.0732	0.0906	0.9394	0.0584	0.0700	0.11142	0.16789
$h = 1$ negative	0.0960	0.0756	0.9407	0.0583	0.0698	0.1134	0.1661
$h = 2$ positive	0.0802	0.0946	0.9119	0.0680	0.0780	0.2872	0.1949
$h = 2$ negative	0.0762	0.1108	0.9119	0.0565	0.0663	0.2888	0.1958
$h = 4$ positive	0.0657	0.1529	0.7512	0.0825	0.0777	0.4138	0.2648
$h = 4$ negative	0.0658	0.1423	0.7499	0.0740	0.0820	0.4140	0.2655
$h = 8$ positive	0.0555	0.0999	0.5172	0.1246	0.0995	0.5543	0.2935
$h = 8$ negative	0.0524	0.0941	0.5077	0.1240	0.0957	0.5526	0.2951
$h = 12$ positive	0.0660	0.1047	0.4121	0.1453	0.1224	0.6450	0.2864
$h = 12$ negative	0.0633	0.0993	0.3973	0.1457	0.1209	0.6444	0.2872

TABLE 6 DM *p*-values for gold returns forecasting comparing the positive only with the negative only multi-scale LPPLS-CI of the G7, and the G7 plus the BRICS.

	G7+BRICS			G7			
Horizon	$T = 100$	$T = 250$	$T = 500$	$T = 100$	$T = 250$	$T = 500$	$T = 1000$
$h = 1$	0.1074	0.09113	0	0.9922	0.1526	0.9160	0.0676
$h = 2$	0.2342	0.08836	0.0414	0.1673	0.1592	0.8387	0.7518
$h = 4$	0.2459	0.1197	0.0890	0.1686	0.1588	0.8207	0.0834
$h = 8$	0.0949	0.1770	0.0629	0.2139	0.1508	0.1679	0.1989
$h = 12$	0.1225	0.1834	0.0816	0.1919	0.1436	0.9630	0.5565

TABLE 7 DM *p*-values for gold returns volatility forecasting comparing the positive only with the negative only multi-scale LPPLS-CI of the G7, and the G7 plus the BRICS.

	G7+BRICS			G7			
Horizon	$T = 100$	$T = 250$	$T = 500$	$T = 100$	$T = 250$	$T = 500$	$T = 1000$
$h = 1$	0.1373	0	0	0.2804	0.0006	0.0559	0.9538
$h = 2$	0.1133	0.3475	0.7645	0.0261	0.1119	0.0026	0.8513
$h = 4$	0.4204	0.5737	0.9343	0.0412	0.1192	0.2340	0.0208
$h = 8$	0.61474	0.8160	0.9081	0.0526	0.1393	0.1441	0.4735
$h = 12$	0.7037	0.8180	0.8810	0.1010	0.1908	0.7720	0.4280

3.4 | Implications of our findings

These findings should be particularly useful for forecasters and investors in the pricing of related derivatives as well as for devising hedging strategies involving gold investments as a safe haven in times booms and busts associated with equity markets of the major economies of the world. Moreover, given that gold returns and volatility tends to act as a proxy for global uncertainty that impacts economic activity,[38,64,65] the high-frequency accurate predictions of the first and second moments of gold prices emanating from equity market bubbles can be incorporated into models of nowcasting[66] to forecast the path of low-frequency real macroeconomic variables. This would help policymakers to design their policy response

to prevent the possible deepening of the recessions, associated with stock market crashes in the first place. From the perspective of an academic, our paper is the first to propose a hypothesis that stock market bubbles matter for predicting movements in moments of gold returns due to its inherent well-established safe haven property, and we provide solid evidence of the same from the perspective of an out-of-sample forecasting, rather than in-sample predictions, thus adding, in some sense, a new predictor to the extensive list of control variables associated with gold market forecasting. Hence, we are able to validate econometrically the intuition that stock market bubbles can be drivers of gold price fluctuations.

4 | CONCLUSION

In this article, our first objective was to detect positive and negative bubbles at short-, medium-, and long-run for the stock markets of the G7 and the BRICS countries by using the multi-scale LPPLS-CI approach. Our findings revealed major crashes and rallies in the 12 stock markets over the period of the 1st week of January, 1973 to the 2nd week of September, 2020. Furthermore, we also observed similar timing of strong (positive and negative) LPPLS-CI values across both the G7 and the BRICS countries, suggesting interconnectedness of the boom-bust cycles in these stock markets. In terms of our second objective, we aim to utilize these indicators to forecast gold returns and its volatility. As we deal with 42 to 72 predictors, the impact of overparameterization, and hence the associated poor out-of-sample performance, cannot be overlooked. Given this, we resort to using an approach involving block means of residuals obtained from the popular LASSO routine, which not only assists us in modeling big data, but also controls for the heavy upper tail of gold returns. We find evidence of the multi-scale indicators, especially when both positive and negative bubbles are considered simultaneously, in accurately forecasting gold returns at short- (one-week-ahead) to medium-run (eight-week-ahead), and also time-varying estimates of gold returns volatility to a lesser extent. Given that forecasting of gold returns is our primary focus, we find that time-varying measures of connectedness of bubbles across the G7, and the G7 plus the BRICS, can also produce qualitatively similar results compared to the case when the individual indicators of the bubbles are considered explicitly.

Given that the idea of the safe haven property of gold is associated with financial market turmoil, in this paper we concentrated on the booms and busts of major stock markets in forecasting gold returns and volatility. Even though, stock market is a well-established leading indicator for macroeconomic and financial variables,[67] we have completely ignored these controls, and can be considered as a limitation of our work. But, one must realize that, finding weekly data for the G7 and BRICS for such variables is not likely to be straight-forward, and we might need innovative proxies in this regard. In addition, in this paper, we only provide point forecasts, when indeed our approach could have been utilized for intervals-based predictions of gold returns and volatility. Keeping the above issues in mind, in future research, it would be interesting to extend our research to other precious metals that have also been identified as safe havens,[68] and even agricultural and nonagricultural commodities, given the evidence of spillover from the equity market, that is, their financialization.[69] Herein, we can also utilize even nonlinear machine learning methods for our purposes. For example, one could use random forests,[70] which, in turn, would help to shed light on potential a nonlinear dependence between gold-market moments and stock market bubbles, as well as any interaction effects between the predictors. Understandably, random forests is a relatively robust econometric method, but whether it would end up producing superior results relative to what we have thus far obtained utilizing linear models is indeed an empirical question for the future.

ACKNOWLEDGMENTS

We would like to thank an anonymous referee, the Associate Editor, and the Editor-in-Chief, Professor Nalini Ravishanker, for many helpful comments. However, any remaining errors are solely ours. The third authors research is partially supported by NSF DMS 2124222.

DATA AVAILABILITY STATEMENT

The data that support the findings of this study are available from the corresponding author upon reasonable request.

ENDNOTES

*The reader is referred to Boubaker et al.[43] for a discussion of all financial market crises going as far back as the 14th century.

†Gold returns in our sample is, unsurprisingly, found to be positively-skewed, with excess kurtosis, resulting in the rejection of the null of normality at the highest level of significance (p-value: 0.00) based on the Jarque-Bera test, which had a value of 4878.11.

‡See, Pierdzioch et al.,[49] Salisu et al.,[6] and Luo et al.[50] for detailed reviews of the literature involving predictors and alternative econometric frameworks used to forecast gold price volatility.

§Note that, a variant of the above method, assisted by bootstrap, was proposed in Chudý et al.[60] But we chose not to employ it, since we are typically aiming for shorter h, and that makes the bootstrap step somewhat unstable.

¶https://www.lbma.org.uk/prices-and-data/precious-metal-prices#/.

#Specifically, UK data is available from January, 1965, and the rest of the G7 starts from January, 1973, while for the BRICS, data of South Africa dates back to January, 1973, but Russian data only begins in February, 1999.

‖The gold returns volatility was also found to be non-normal with a large Jarque-Bera test statistic (of 2,485,559.00), and a corresponding p-value of 0.00.

**Additional results with a different choice of λ and volatilities estimated with an alternative bandwidth b_n, other than 0.25, are available upon request from the authors. However, the general findings to those reported in the paper remains qualitatively similar.

††The reader is referred to the Appendix of our paper for further technical details.

ORCID

Sayar Karmakar https://orcid.org/0000-0002-4841-2069

REFERENCES

1. Pierdzioch C, Risse M, Rohloff S. On the efficiency of the gold market: results of a real-time forecasting approach. *Int Rev Financ Anal*. 2014;32:95-108.
2. Pierdzioch C, Risse M, Rohloff S. The international business cycle and gold-price fluctuations. *Q Rev Econ Finance*. 2014;54(2):292-305.
3. Pierdzioch C, Risse M, Rohloff S. A real-time quantile-regression approach to forecasting gold returns under asymmetric loss. *Res Policy*. 2015;45(C):299-306.
4. Pierdzioch C, Risse M, Rohloff S. Forecasting gold-price fluctuations: a real-time boosting approach. *Appl Econ Lett*. 2015;22(1):46-50.
5. Pierdzioch C, Risse M, Rohloff S. A quantile-boosting approach to forecasting gold returns. *North Am J Econom Finance*. 2016;35:38-55.
6. Salisu AA, Gupta R, Bouri E, et al. The role of global economic conditions in forecasting gold market volatility: evidence from a GARCH-MIDAS approach. *Res Int Bus Financ*. 2020;54:101308.
7. Aye GC, Gupta R, Hammoudeh S, Kim W-J. Forecasting the price of gold using dynamic model averaging. *Int Rev Financ Anal*. 2015;41(C):257-266.
8. Hassani H, Silva ES, Gupta R, Segnon MK. Forecasting the price of gold. *Appl Econ*. 2015;47(39):4141-4152.
9. Sharma SS. Can consumer price index predict gold price returns? *Econ Model*. 2016;55:269-278.
10. Gupta R, Majumdar A, Pierdzioch C, Wohar ME. Do terror attacks predict gold returns? Evidence from a quantile-predictive-regression approach. *Q Rev Econ Finance*. 2017;65(C):276-284.
11. Bonato M, Demirer R, Gupta R, Pierdzioch C. Gold futures returns and realized moments: a forecasting experiment using a quantile-boosting approach. *Res Policy*. 2018;57:196-212.
12. Nguyen DBB, Prokopczuk M, Wese Simen C. The risk premium of gold. *J Int Money Financ*. 2019;94:140-159.
13. Dichtl H. Forecasting excess returns of the gold market: can we learn fromstock market predictions? *J Commod Mark*. 2020;19:100106.
14. Plakandaras V, Ji Q. Intrinsic decompositions in gold forecasting. *J Commod Mark*. 2022;28:100245. doi:10.1016/j.jcomm.2022.100245
15. Bahloul W, Balcilar M, Cunado J, Gupta R. The role of economic and financial uncertainties in predicting commodity futures returns and volatility: evidence from a nonparametric causality-in-quantiles test. *J Multinatl Financ Manag*. 2018;45:52-71.
16. Baur DG, Lucey BM. Is gold a hedge or a safe haven? An analysis of stocks, bonds and gold. *Financ Rev*. 2010;45:217-229.
17. Baur DG, McDermott TK. Is gold a safe haven? International evidence. *J Bank Financ*. 2010;34:1886-1898.
18. Reboredo JC. Is gold a safe haven or a hedge for the US dollar? Implications for risk management. *J Bank Financ*. 2013;37(8):2665-2676.
19. Reboredo JC. Is gold a hedge or safe haven against oil price movements? *Res Policy*. 2013;38(2):130-137.
20. Agyei-Ampomah S, Gounopoulos D, Mazouz K. Does gold offer a better protection against sovereign debt crisis than other metals? *J Bank Financ*. 2014;40:507-521.
21. Gürgün G, Ünalmis I. Is gold a safe haven against equity market investment in emerging and developing countries? *Financ Res Lett*. 2014;11:341-348.
22. Beckmann J, Berger T, Czudaj R. Does gold act a hedge or safe haven for stocks? A smooth transition approach. *Econ Model*. 2015;48:16-24.
23. Low RKY, Yao Y, Faff R. Diamonds vs. precious metals: what shines brightest in your investment portfolio? *Int Rev Financ Anal*. 2016;43:1-14.
24. Balcilar M, Demirer R, Gupta R, Wohar ME. The effect of global and regional stock market shocks on safe haven assets. *Struct Chang Econ Dyn*. 2020;54:297-308.
25. Ji Q, Zhang D, Zhao Y. Searching for safe-haven assets during the COVID-19 pandemic. *Int Rev Financ Anal*. 2020;71:101526.
26. Tiwari AK, Aye GC, Gupta R, Gkillas K. Gold-oil dependence dynamics and the role of geopolitical risks: evidence from a Markov-switching time-varying copula model. *Energy Econ*. 2020;88:104748.
27. Lahiani A, Mefteh-Wali S, Vasbieva DG. The safe-haven property of precious metal commodities in the COVID-19 era. *Res Policy*. 2021;74:102340.
28. Johansen A, Ledoit O, Sornette D. Crashes as critical points. *Int J Theoret Appl Finance*. 2000;2:219-255.
29. Johansen A, Sornette D, Ledoit O. Predicting financial crashes using discrete scale invariance. *J Risk*. 1999;1(4):5-32.

30. Sornette D. *Why Stock Markets Crash: Critical Events in Complex Financial Systems*. Princeton University Press; 2003.
31. Demirer R, Demos G, Gupta R, Sornette D. On the predictability of stock market bubbles: evidence from LPPLS confidence multi-scale indicators. *Quant Financ*. 2019;19(5):843-858.
32. Caporin M, Gupta R, Ravazzolo F. Contagion between real estate and financial markets: a Bayesian quantile-on-quantile approach. *North Am J Econom Finance*. 2021;55:101347.
33. Caporin M, Pelizzon L, Ravazzolo F, Rigobon R. Measuring sovereign contagion in Europe. *J Financ Stab*. 2018;34:150-181.
34. Campbell JY, Shiller RJ. The dividend-price ratio and expectations of future dividends and discount factors. *Rev Financ Stud*. 1988;1(3):195-228.
35. Çepni O, Guney IE, Gupta R, Wohar ME. The role of an aligned investor sentiment index in predicting bond risk premia of the United States. *J Financ Mark*. 2020;51(1):100541.
36. Hollstein F, Prokopczuk J, Tharann B, Wese Simen C. Predictability in commodity markets: evidence from more than a century. *J Commod Mark*. 2021;24(C):100171.
37. Koki C, Leonardos S, Piliouras G. Exploring the predictability of cryptocurrencies via Bayesian hidden Markov models. *Res Int Bus Financ*. 2022;59(1):101554.
38. Salisu AA, Cunado J, Gupta R. Geopolitical risks and historical exchange rate volatility of the BRICS. *Int Rev Econ Financ*. 2022;77:179-190.
39. Balcilar M, Gupta R, Jooste C, Wohar ME. Periodically collapsing bubbles in the South African stock market? *Res Int Bus Financ*. 2016;38:191-201.
40. Zhang Q, Sornette D, Balcilar M, Gupta R, Ozdemir ZA, Yetkiner H. LPPLS bubble indicators over two centuries of the S&P 500 index. *Phys A Stat Mech Appl*. 2016;458(C):126-139.
41. Sornette D, Cauwels P, Smilyanov G. Can we use volatility to diagnose financial bubbles? Lessons from 40 historical bubbles. *Quant Finance Econom*. 2018;2(1):486-590.
42. Müller UA, Dacorogna MM, Davé RD, Olsen RB, Pictet OV. Volatilities of different time resolutions–analyzing the dynamics of market components. *J Empir Financ*. 1997;4:213-239.
43. Boubaker H, Cunado J, Gil-Alana LA, Gupta R. Global crises and gold as a safe haven: evidence from over seven and a half centuries of data. *Phys A Stat Mech Appl*. 2020;540:123093.
44. Bouri E, Demirer R, Gupta R, Sun X. The predictability of stock market volatility in emerging economies: relative roles of local, regional, and global business cycles. *J Forecast*. 2020;39(6):957-965.
45. Das S, Demirer R, Gupta R, Mangisa S. The effect of global crises on stock market correlations: evidence from scalar regressions via functional data analysis. *Struct Chang Econ Dyn*. 2019;50(C):132-147.
46. Tibshirani R. Regression shrinkage and selection via the lasso. *J R Stat Soc Ser B*. 1996;58:267-288.
47. Karmakar S, Chudý M, Wu WB. Long-term prediction intervals with many covariates. *J Time Ser Anal*. 2021;43:52-7609. doi:10.1111/jtsa.12629
48. Baur DG. Asymmetric volatility in the gold market. *J Altern Invest*. 2012;14:26-38.
49. Pierdzioch C, Risse M, Rohloff S. A boosting approach to forecasting the volatility of gold-price fluctuations under flexible loss. *Res Policy*. 2016;47:95-107.
50. Luo J, Demirer R, Gupta R, Ji Q. Forecasting oil and gold volatilities with sentiment indicators under structural breaks. *Energy Econ*. 2022;105:105751.
51. Karmakar S, Roy A. Bayesian modelling of time-varying conditional heteroscedasticity. *Bayesian Anal*. 2021;16(4):1157-1185.
52. Karmakar S, Demirer R, Gupta R. Bitcoin mining activity and volatility dynamics in the power market? *Econ Lett*. 2021;209:110111.
53. Filimonov V, Sornette D. A stable and robust calibration scheme of the log-periodic power law model. *Phys A Stat Mech Appl*. 2013;392(17):3698-3707.
54. Sornette D, Demos G, Zhang Q, Cauwels P, Filimonov V, Zhang Q. Real-time prediction and post-mortem analysis of the Shanghai 2015 stock market bubble and crash. *J Investment Strateg*. 2015;4:77-95.
55. Zhou Z, Xu Z, Wu WB. Long-term prediction intervals of time series. *IEEE Trans Inf Theory*. 2010;56:1436-1446.
56. Stărică C. *Is GARCH(1,1) as good a model as the accolades of the Nobel prize would imply? Econometrics 0411015*. University Library of Munich; 2003.
57. Fryzlewicz P, Sapatinas T, Rao SS. Normalized least-squares estimation in time-varying arch models. *Ann Stat*. 2008;36:742-786.
58. Karmakar S, Richter S, Wu WB. Simultaneous inference for time-varying models. *J Econ*. 2022;227(2):408-428. doi:10.1016/j.jeconom.2021.03.002
59. Müller UK, Watson MW. Measuring uncertainty about long-run predictions. *Rev Econ Stud*. 2016;83:1711-1740.
60. Chudý M, Karmakar S, Wu WB. Long-term prediction intervals of economic time series. *Empir Econ*. 2020;58:191-222.
61. Clark TD, West KD. Approximately normal tests for equal predictive accuracy in nested benchmark/rival model. *J Econ*. 2007;138:29-311.
62. Antonakakis N, Chatziantoniou I, Gabauer D. Refined measures of dynamic connectedness based on time-varying parameter vector autoregressions. *J Risk Financ Manage*. 2020;13:84.
63. Diebold FX, Mariano RS. Comparing predictive accuracy. *J Bus Econ Stat*. 1995;13(3):253-263.
64. Çepni O, Dul W, Gupta R, Wohar ME. The dynamics of U.S. REITs returns to uncertainty shocks: a proxy SVAR approach. *Res Int Bus Financ*. 2021;58(C):101433.
65. Piffer M, Podstawski M. Identifying uncertainty shocks using the price of gold. *Econ J*. 2017;128(616):3266-3284.
66. Bańbura M, Giannone D, Reichlin L. Nowcasting. In: Clements MP, Hendry DF, eds. *The Oxford Handbook on Economic Forecasting*. Oxford University Press; 2011:63-90.

67. Stock JH, Watson MW. Forecasting output and inflation: the role of asset prices. *J Econ Lit*. 2003;41(3):788-829.
68. Salisu AA, Gupta R, Ntyikwe S, Demirer R. Gold and the Global Financial Cycle. *Quant Finance Econom*. 2023;7(3):475-490.
69. Bonato M. Realized correlations, betas and volatility spillover in the agricultural commodity market: what has changed? *J Int Financ Mark Inst Money*. 2019;62:184-202.
70. Breiman L. Random forests. *Mach Learn*. 2001;45(1):5-32.
71. Diebold FX, Yilmaz K. Measuring financial asset return and volatility spillovers, with application to global equity markets. *Econ J*. 2009;119(534):158-171.
72. Diebold FX, Yilmaz K. Better to give than to receive: predictive directional measurement of volatility spillovers. *Int J Forecast*. 2012;28(1):57-66.
73. Diebold FX, Yilmaz K. On the network topology of variance decompositions: measuring the connectedness of financial firms. *J Econ*. 2014;182(1):119-134.
74. Koop G, Pesaran MH, Potter SM. Impulse response analysis in nonlinear multivariate models. *J Econ*. 1996;74(1):119-147.
75. Pesaran MH, Shin Y. Generalized impulse response analysis in linear multivariate models. *Econ Lett*. 1998;58(1):17-29.

How to cite this article: Gabauer D, Gupta R, Karmakar S, Nielsen J. Stock market bubbles and the forecastability of gold returns and volatility. *Appl Stochastic Models Bus Ind*. 2024;1-19. doi: 10.1002/asmb.2887

APPENDIX. TOTAL CONNECTEDNESS INDEX

We compute the dynamic total connectedness index (TCI) for the six bubble indicators under the cases of the G7 and the G7 plus the BRICS using the time-varying parameter vector autoregressive (TVP-VAR) based connectedness approach of Antonakakis et al.,[62] which is an extension of the original constant parameter VAR-based approach of Diebold and Yilmaz.[71–73] Thus, we first estimate the following TVP-VAR model with a lag length of one as suggested by the Bayesian information criterion. The resulting TVP-VAR model can be outlined as follows:

$$\boldsymbol{z}_t = \boldsymbol{B}_t \boldsymbol{z}_{t-1} + \boldsymbol{u}_t, \qquad \boldsymbol{u}_t \sim N(\boldsymbol{0}, \boldsymbol{S}_t), \tag{A1}$$

$$vec(\boldsymbol{B}_t) = vec(\boldsymbol{B}_{t-1}) + \boldsymbol{v}_t, \qquad \boldsymbol{v}_t \sim N(\boldsymbol{0}, \boldsymbol{R}_t), \tag{A2}$$

where $\boldsymbol{z}_t$, $\boldsymbol{z}_{t-1}$ and $\boldsymbol{u}_t$ are $k \times 1$ dimensional vectors, denoting the specific bubble indicator in t, $t-1$, and the corresponding error term, respectively. $\boldsymbol{B}_t$ and $\boldsymbol{S}_t$ are $k \times k$ dimensional matrices illustrating the time-varying VAR coefficients and the time-varying variance-covariances while $vec(\boldsymbol{B}_t)$ and $\boldsymbol{v}_t$ are $k^2 \times 1$ dimensional vectors and $\boldsymbol{R}_t$ denotes a $k^2 \times k^2$ dimensional matrix.

As the generalised forecast error variance decomposition (GFEVD) of Koop et al.[74] and Pesaran and Shin[75] rests on the vector moving average (VMA) coefficients, we apply the Wold representation theorem to transform the TVP-VAR to its TVP-VMA process by the following equality: $\boldsymbol{z}_t = \sum_{i=1}^{p} \boldsymbol{B}_{it} \boldsymbol{z}_{t-i} + \boldsymbol{u}_t = \sum_{j=0}^{\infty} \boldsymbol{A}_{jt} \boldsymbol{u}_{t-j}$. The GFEVD, $\tilde{\psi}^g_{ij,t}(H)$, stands for the influence series j has on series i in terms of its forecast error variance share and is computed by

$$\psi^g_{ij,t}(H) = \frac{S^{-1}_{ii,t} \sum_{t=1}^{H-1} (\boldsymbol{\iota}_i' \boldsymbol{A}_t \boldsymbol{S}_t \boldsymbol{\iota}_j)^2}{\sum_{j=1}^{k} \sum_{t=1}^{H-1} (\boldsymbol{\iota}_i \boldsymbol{A}_t \boldsymbol{S}_t \boldsymbol{A}_t' \boldsymbol{\iota}_i)} \qquad \tilde{\psi}^g_{ij,t}(H) = \frac{\psi^g_{ij,t}(H)}{\sum_{j=1}^{k} \phi^g_{ij,t}(H)},$$

with $\sum_{j=1}^{k} \tilde{\psi}^g_{ij,t}(H) = 1$, $\sum_{i,j=1}^{k} \tilde{\psi}^g_{ij,t}(H) = k$, where H stands for the forecast horizon, and $\boldsymbol{\iota}_i$ for a zero vector with unity on the ith position.

Subsequently, the TCI can be constructed. This connectedness measure indicates the degree of network interconnectedness:

$$TCI = \frac{\sum_{i,j=1, i \neq j}^{k} \tilde{\psi}^g_{ij,t}(H)}{\sum_{i,j=1}^{k} \tilde{\psi}^g_{ij,t}(H)} \qquad 0 \leq C^g_t(H) \leq 1. \tag{A3}$$

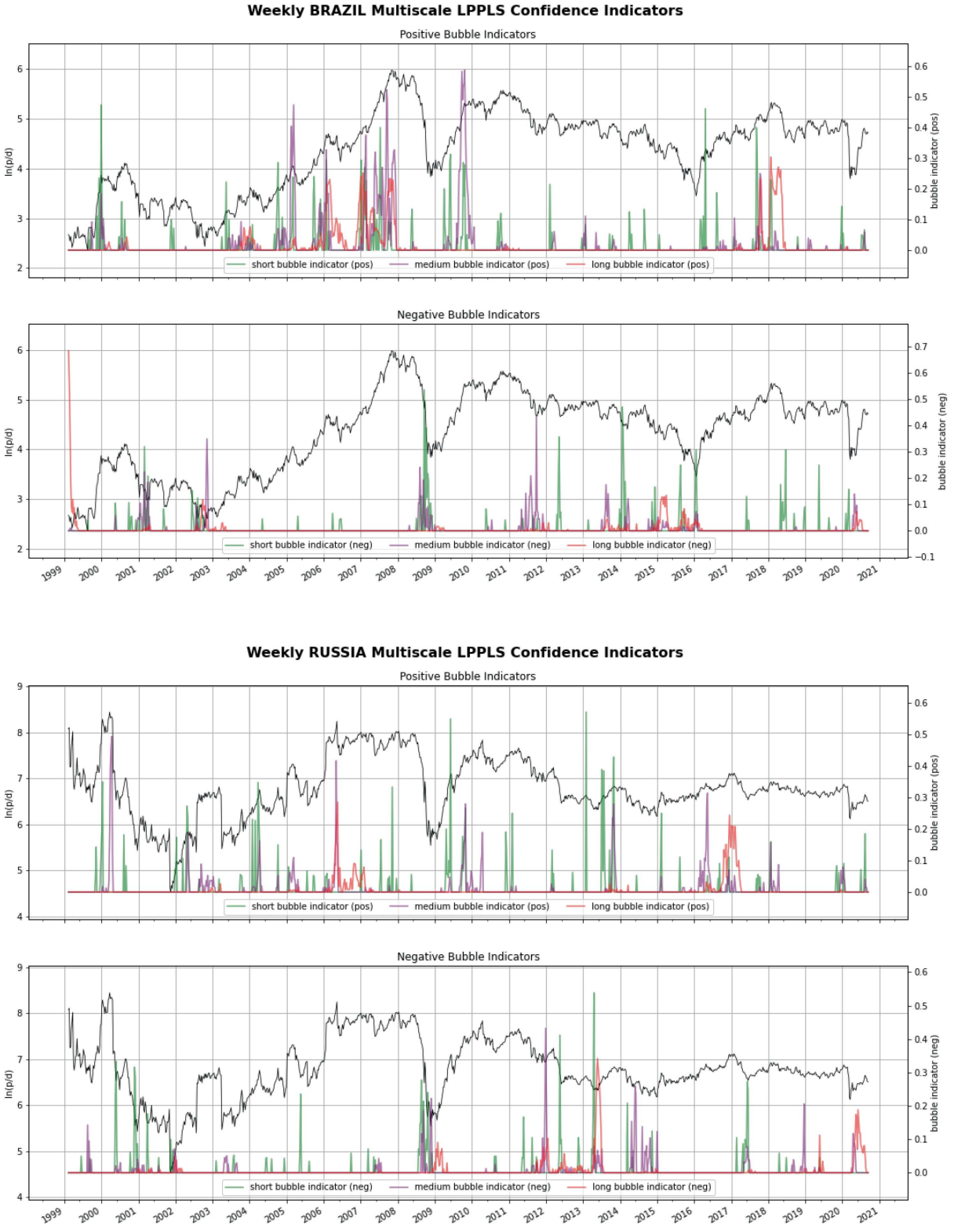

FIGURE A1 BRICS weekly multi-scale LPPLS-CI.

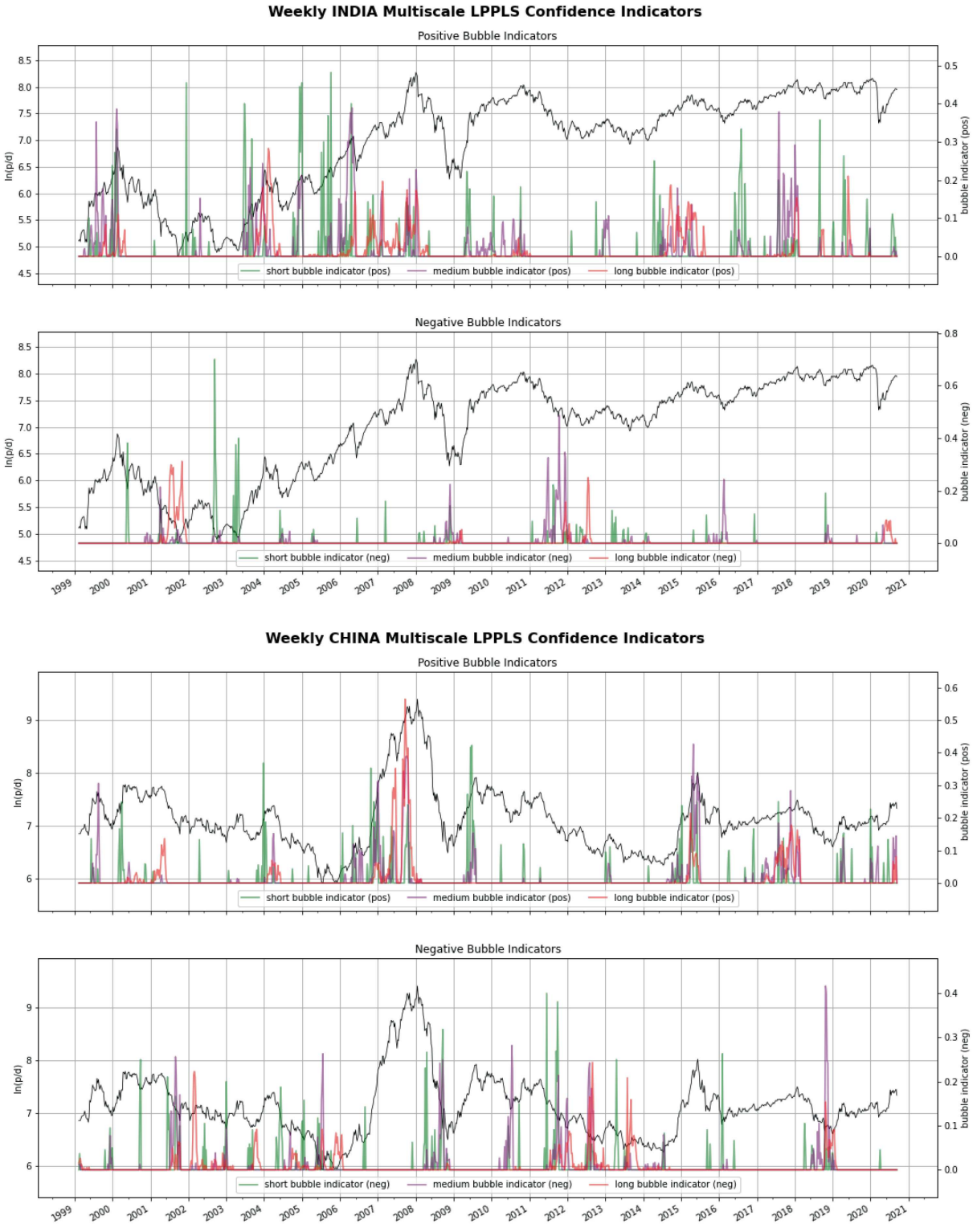

FIGURE A2 BRICS weekly multi-scale LPPLS-CI.

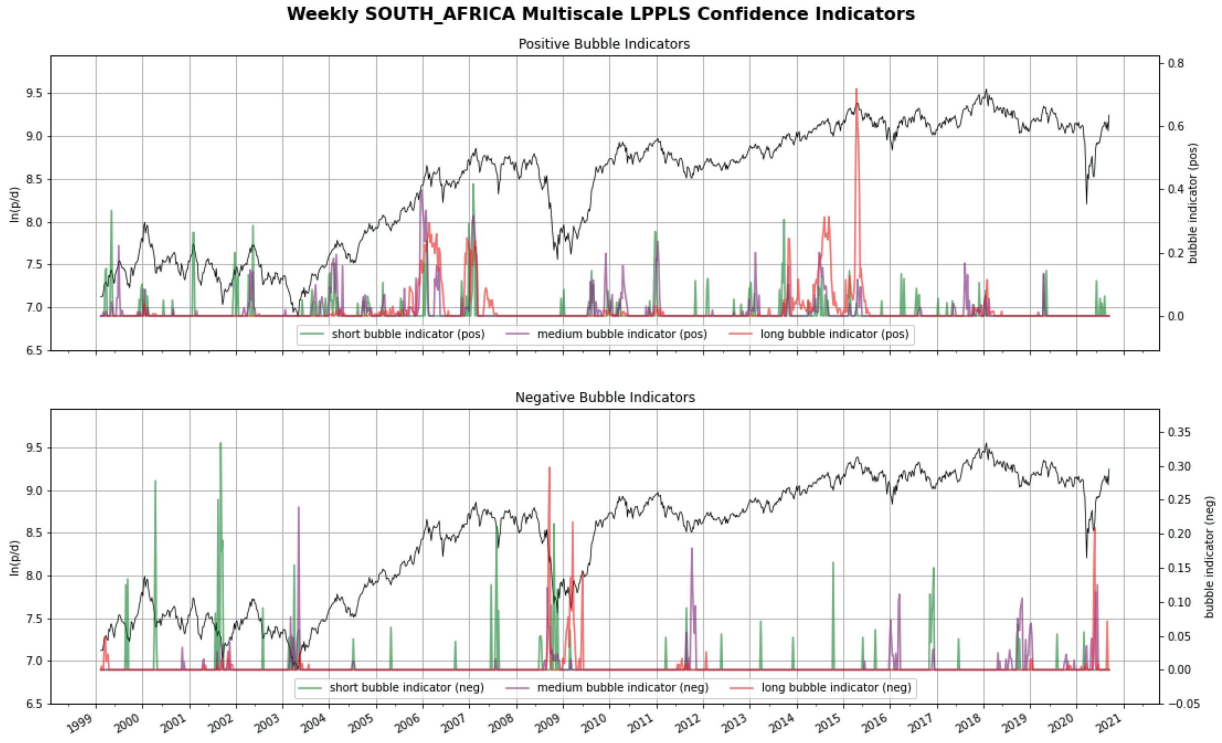

FIGURE A3 BRICS weekly multi-scale LPPLS-CI.